

## SUPPLEMENTARY INFORMATION

---

### On-Surface Ullmann Polymerization via Intermediate Organometallic Networks on Ag(111)

Johanna Eichhorn,<sup>a,b,c</sup> Thomas Strunskus,<sup>d</sup> Atena Rastgoo-Lahrood,<sup>a,b,c</sup> Michael Schmittel,<sup>e</sup> and Markus Lackinger<sup>a,b,f,\*</sup>

<sup>a</sup>Department of Physics Technische Universität München, James-Frank-Str. 1, 85748 Garching, Germany.

<sup>b</sup>Center for NanoScience (CeNS), Schellingstrasse 4, 80799 Munich, Germany.

<sup>c</sup>TUM School of Education, Technische Universität München, Marsstraße 12, 80335 München, Germany.

<sup>d</sup>Institute for Materials Science – Multicomponent Materials, Christian-Albrechts-Universität zu Kiel, Kaiserstr. 2, 24143 Kiel, Germany.

<sup>e</sup>Center of Micro- and Nanochemistry and Engineering, Organische Chemie I, Universität Siegen, Adolf-Reichwein-Str. 2, 57068 Siegen, Germany.

<sup>f</sup>Deutsches Museum, Museumsinsel 1, 80538, Munich, Germany.

Tel: +49 89 2179-605; E-mail markus@lackinger.org

#### Table of Content

1.	Materials and methods .....	2
1.1	Experimental details: STM .....	2
1.2	Experimental details: XPS .....	3
1.3	Synthesis of BIB .....	3
2.	Additional data .....	4
2.1	STM data.....	4
2.2	DFT calculations.....	4
	References.....	5

# 1. Materials and methods

## 1.1 Experimental details: STM

All experiments were conducted with a home-built Scanning-Tunneling-Microscope (STM) under ultra-high vacuum (UHV) conditions with a base pressure below  $2 \times 10^{-10}$  mbar. All STM data were recorded at room temperature using a SPM 100 control electronics from RHK using the XPM Pro 2.0.1.5 software. Lattice parameters and intermolecular distances were derived from STM images with an accuracy of  $\sim 5\%$  after calibration with atomically resolved topographs of highly oriented pyrolytic graphite(001). Tunneling parameters of all STM images are summarized in Table 1.

Single crystal Ag(111) surfaces were prepared by cycles of  $\text{Ar}^+$ -ion sputtering at 500 eV and annealing at 500 °C for 40 minutes. The cleanliness of the substrate was verified by STM imaging prior to deposition.

Synthesis details and characterization of 1,3-bis(*p*-bromophenyl)-5-(*p*-iodophenyl)benzene (BIB) will be published elsewhere. BIB was deposited by means of a home-built Knudsen cell with crucible temperatures of 126 °C to 168 °C. During deposition the Ag(111) substrate was either held at room temperature or heated above 125 °C. No influence of the deposition rate on the morphology of the organometallic networks could be discerned.

**Table 1.** Tunneling parameters of all depicted STM images.

Figure	Tunneling parameters
1	a) -0.90 V, 8.0 pA
	b) +1.1 V, 3.9 pA
	c) -0.30 V, 10 pA
	d) +4.0 V, 5.5 pA
2	b) +0.80 V, 11 pA
	c) +0.90 V, 7.8 pA
	d) +0.20 V, 7.8 pA
3	a) -1.9 V, 25 pA
	b) +3.9 V, 4.6 pA
	c) +3.9 V, 4.6 pA
	d) +2.6 V, 5.5 pA

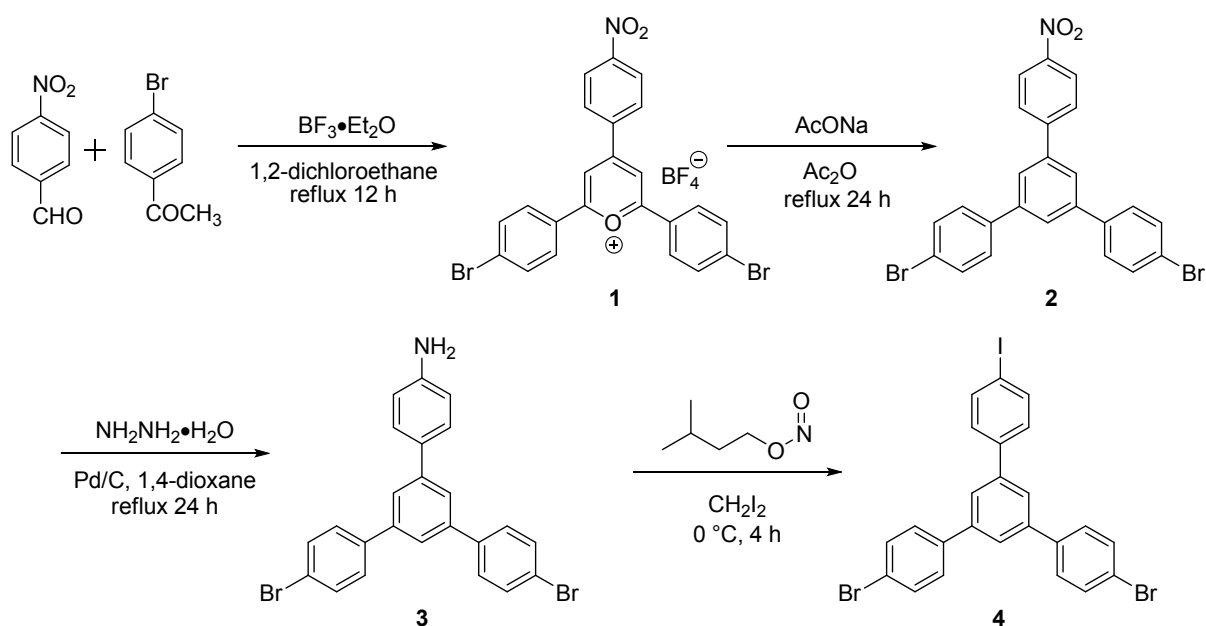
## 1.2 Experimental details: XPS

XPS measurements were carried out in a Prevac UHV system at the HESGM beamline at Helmholtz-Zentrum Berlin. The preparation chamber of the UHV system was equipped with facilities for sample sputtering and heating. The sample preparation was similar to the STM experiments. Bromine 3d XP spectra were acquired with a Scienta R3000 electron analyzer at normal electron emission using an excitation energy of 450 eV and a pass energy of 50 eV. The binding energy of Ag 3d<sub>5/2</sub> at 368.3 eV was used as an internal energy reference. A linear background was subtracted from all spectra.

## 1.3 Synthesis of BIB

The synthesis of 1,3-bis(*p*-bromophenyl)-5-(*p*-iodophenyl)benzene (BIB) (**4**) was achieved in four steps following a general strategy for unsymmetrically substituted 1,3,5-triphenylbenzenes as outlined by Mikroyannidis.<sup>1</sup> At first, triphenylpyrylium salt **1** was prepared in an acid catalyzed condensation between 4-nitrobenzaldehyde and 4-bromoacetophenone in 1,2-dichloroethane. Thereafter, **1** was converted to 1,3,5-triphenylbenzene **2** by heating in acetic anhydride in presence of sodium acetate. Using a palladium catalyzed reduction 1-(*p*-aminophenyl)-3,5-bis(*p*-bromophenyl)benzene (**3**) was afforded from **2**. Finally, the iodination was accomplished using isoamyl nitrite in diiodomethane at 0 °C.

**Scheme 1.** Synthetic route to 1,3-bis(*p*-bromophenyl)-5-(*p*-iodophenyl)benzene (**4**).



## 2. Additional data

### 2.1 STM data

RT deposition of BIB and subsequent annealing at 155 °C already resulted in the formation of individual covalent cross-links. Those are clearly identified by the reduced length of the center-to-center distance of connected molecules, and appear with uniform STM contrast as opposed to the organometallic bonds, where the silver atoms appears as small protrusion.

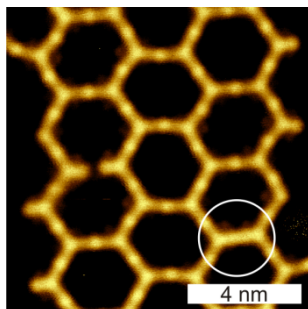


**Figure S1.** STM image acquired after RT deposition of BIB onto Ag(111) and subsequent tempering at 155 °C. Most of the molecules are interconnected by organometallic bonds, where the silver atom appears as small protrusion. Yet, single covalent bonds with reduced length are already observed, an example is indicated by the white circle.

In STM images of both organometallic and covalent networks regularly arranged bright dots are clearly discernible within the pores. These features are assigned as split off halogens, because they have never been observed on clean Ag(111) surface and the size is in accordance. A distinction between bromine and iodine based on the STM contrast, however, was not possible. The STM images in Fig. S2 depict adsorbed halogens in the pores of an (a) organometallic and (b) / (c) covalent network, respectively. The STM images in Fig. S2(b) and (c) were acquired from the same sample area, yet with different tunneling parameters. The differences in STM contrast especially of the halogens suggest a distinct dependence on the imaging parameters.

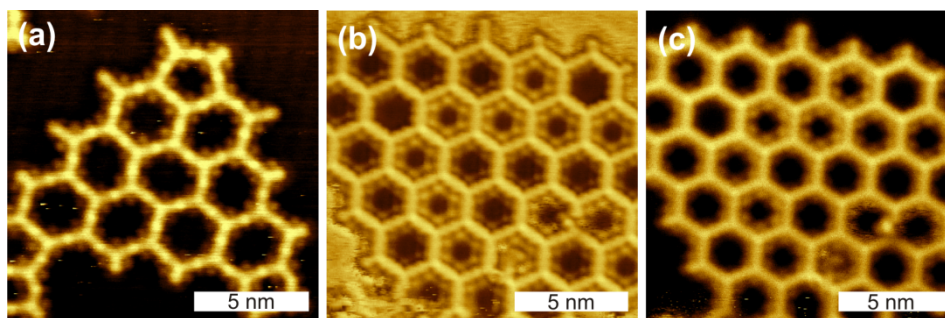


**Figure S2.** STM images of BIB derived (a) organometallic and (b)+(c) covalent networks on Ag(111). (a) was acquired after deposition at 125 °C, whereas the sample in (b)+(c) was prepared by deposition at 150 °C and subsequent tempering to 250 °C. In both networks the split off halogens are clearly discernible at defined positions within the pores. (tunneling parameters: (a) 6.2 pA, +0.50 V, (b) 9.2 pA, +1.6 V, (c) +4.6 pA, 3.9 V)

## 2.2 DFT calculations

DFT gas phase calculations were conducted for comparing the bond lengths of anticipated structures with experimental data. Therefore, the geometries of covalent dimers and organometallic complexes were optimized with Gaussian03 applying standard convergence criteria. For hydrogen, carbon, and bromine a B3LYP functional and a 6-31G\* basis set was used, whereas a LanL2DZ basis set was chosen for silver.<sup>2</sup> The substrate influence was mimicked by fixing the dihedral angles for a planar conformation. In accordance with these calculations, the bond length difference between covalent and organometallic cross-links amounts to 0.27 nm (cf. Fig. S2). This length difference is large enough to unambiguously distinguish organometallic from covalent bonds in STM experiments.

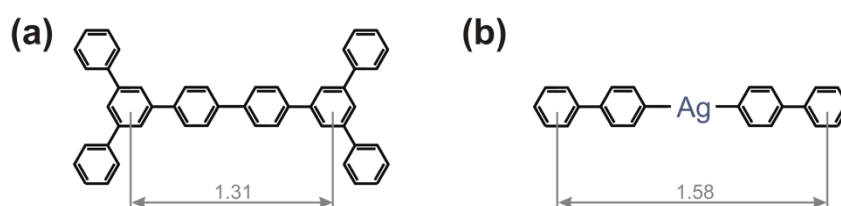


**Figure S3.** DFT geometry optimized structures of a covalent dimer (a) and the corresponding organometallic complex (b) in the gas phase. All distances are given in nm.

Furthermore, a fully brominated covalent dimer was optimized to estimate length differences between still brominated and already debrominated molecular lobes. The distance from the outermost phenyl ring of the quarterphenyl backbone to the peripheral bromine atom is 0.77 nm. This is 0.20 nm longer than the distance to the outermost carbon atom (Fig. S3). Based on

these calculations, we anticipate that brominated and debrominated molecular lobes can be clearly distinguished in STM images by the apparent length of the respective molecular lobe.

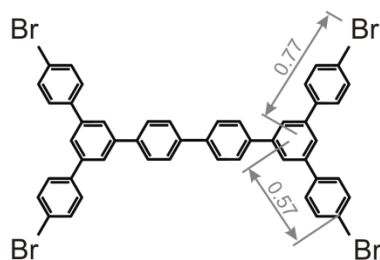


**Figure S4.** DFT geometry optimized structure of a fully brominated covalent dimer in the gas phase. All distances are given in nm.

## References

- [1] J. A. Mikroyannidis, *J. Polym. Sci., Part A: Polym. Chem.* **1999**, *37*, 15.
- [2] Frisch, M. J.; Trucks, G. W.; Schlegel, H. B.; Scuseria, G. E.; Robb, M. A.; Cheeseman, J. R.; Montgomery, J. A.; Vreven, T.; Kudin, K. N.; Burant, J. C.; Millam, J. M.; Iyengar, S. S.; Tomasi, J.; Barone, V.; Mennucci, B.; Cossi, M.; Scalmani, G.; Rega, N.; Petersson, G. A.; Nakatsuji, H.; Hada, M.; Ehara, M.; Toyota, K.; Fukuda, R.; Hasegawa, J.; Ishida, M.; Nakajima, T.; Honda, Y.; Kitao, O.; Nakai, H.; Klene, M.; Li, X.; Knox, J. E.; Hratchian, H. P.; Cross, J. B.; Bakken, V.; Adamo, C.; Jaramillo, J.; Gomperts, R.; Stratmann, R. E.; Yazyev, O.; Austin, A. J.; Cammi, R.; Pomelli, C.; Ochterski, J. W.; Ayala, P. Y.; Morokuma, K.; Voth, G. A.; Salvador, P.; Dannenberg, J. J.; Zakrzewski, V. G.; Dapprich, S.; Daniels, A. D.; Strain, M. C.; Farkas, O.; Malick, D. K.; Rabuck, A. D.; Raghavachari, K.; Foresman, J. B.; Ortiz, J. V.; Cui, Q.; Baboul, A. G.; Clifford, S.; Cioslowski, J.; Stefanov, B. B.; Liu, G.; Liashenko, A.; Piskorz, P.; Komaromi, I.; Martin, R. L.; Fox, D. J.; Keith, T.; Al-Laham, M. A.; Peng, C. Y.; Nanayakkara, A.; Challacombe, M.; Gill, P. M. W.; Johnson, B.; Chen, W.; Wong, M. W.; Gonzalez, C.; Pople, J. A. *Gaussian 03*, Gaussian, Inc., Wallingford, CT: **2004**.